Bhargav Amruth (Orcid ID: 0000-0002-1793-8340)
Manthiram Arumugam (Orcid ID: 0000-0003-0237-9563)

Article category: Full Paper
Subcategory: Metal-sulfur Batteries

2,5-Dimercapto-1,3,4-thiadiazole (DMCT)-based Polymers for Rechargeable Metal-sulfur Batteries

*Amruth Bhargav and Arumugam Manthiram**

Mr. A. Bhargav, Prof. A. Manthiram
Materials Science and Engineering Program & Texas Materials Institute
The University of Texas at Austin, Austin, TX 78712, USA
E-mail: manth@austin.utexas.edu (A. Manthiram)

Keywords: metal-sulfur batteries, organosulfur batteries, organopolysulfide, 2,5-dimercapto-1,3,4-thiadiazole, electrochemistry

Organosulfur materials are a sustainable alternative to the present-day layered oxide cathodes in lithium-based batteries. One such organosulfur material that was intensely explored from the 1990s to early 2010s is 2,5-dimercapto-1,3,4-thiadiazole (DMCT). However, research interest declined as the electrode reactions with DMCT were assumed to be too sluggish to be practical. Armed with the advances in metal-sulfur batteries, we revisit DMCT-based materials in the form of poly[tetrathio-2,5-(1,3,4-thiadiazole)], referred to as pDMCT-S. With an appropriate choice of electrode design and electrolyte, pDMCT-S cathode paired with a Li-metal anode shows a capacity of 715 mA h g^{-1} and a Coulombic efficiency of 97.7 % at a C/10 rate, thus quelling the concerns of sluggish reactions. Surprisingly, pDMCT-S displays significantly improved long-term cyclability compared to a sulfur cathode. Investigations into the origin of the stability reveals that the discharge product Li-DMCT in its mesomeric form can strongly bind to polysulfides, preventing their dissolution into the electrolyte and shuttling. This unique mechanism solves a critical problem faced by sulfur cathodes. Encouragingly, this mechanism results in a stable performance of pDMCT-S with Na-metal cells as well. This study opens the potential for exploring other organic materials that have inherent polysulfide sequestering capabilities, enabling long-life metal-sulfur batteries.

1. Introduction

The fast-paced development of high-energy-density lithium-ion (Li-ion) batteries over the last three decades have revolutionized modern human life with portable devices and electric transport.[1,2] The demand for Li-ion batteries is expected to exceed 2,000 GWh annually by 2030.[3] Such a steep demand would put a strain on the production of currently used layered oxide cathode materials rendering them an unsustainable option for the future.[4] Metal-sulfur batteries and their subset metal-organosulfur batteries offer a sustainable solution to this crisis owing to the large abundance of raw materials and their environmental benignity.[5]

Organosulfur compounds consist of linear polysulfide chains attached to organic functional groups either as end caps or as the central backbone.[6,7] Attaching organic groups to the inorganic sulfur alters the redox potential of sulfur. It also affects other properties critical for battery materials, such as electronic conductivity, ionic conductivity, and solubility in the electrolyte.[6–10] Redox-active organosulfur compounds were first introduced in the late 1980s by Visco and others.[8,11–15] These reports demonstrated the high reversibility of the disulfide-thiolate redox couple. One of the compounds introduced was the polymer based on 2,5-dimercapto-1,3,4-thiadiazole (DMCT). The thiolate form of DMCT was shown to convert to the polymeric disulfide form, namely poly[dithio-2,5-(1,3,4-thiadiazole)] (pDMCT) *in-situ* through a 2-electron transfer, thus affording a theoretical specific capacity of 362 mA h g^{-1}.

Following these initial reports, DMCT was explored with high fervor from the 1990s to early 2010s.[14–20] Early research concluded that the conductivity of DMCT was low and the conversion reaction was kinetically sluggish.[15,16] To overcome this perceived challenge, composites of DMCT were made with electron- and ion-conductive agents such as carbon fibers,[21] graphene,[22] polyaniline,[16,21] poly(3,4-ethylenedioxythiophene) (PEDOT),[18] and PEDOT-polystyrene sulfonate mixtures.[19] These strategies improved the extractable capacity from the cell. However, the cyclability of these cells was typically below 50 cycles. As the rechargeability of DMCT appeared poor, the interest in pursuing DMCT as an active material waned. It is important to note that most of these studies employed carbonate-based electrolytes. It is now well known that the carbonate-based electrolytes are susceptible to nucleophilic attack by the radicals formed during the operation of sulfur/organosulfur cathodes.[23] Additionally, carbonate-based electrolytes are also known to be unstable with alkali-metal anodes.[24,25] Therefore, the poor performance obtained in the early reports was misattributed to sluggish charge transfer and kinetics, while the inappropriate choice of electrolyte was the true culprit. The improved stability of DMCT in an ether-based electrolyte that is commonly used with sulfur cathodes today was examined by Abruña's group in 2012.[20] Despite using a favorable electrolyte, the reported capacity was low (< 50 % utilization) and the cycle life was limited to 20 cycles. Beyond this encouraging result, we found no further follow-up research to the best of our knowledge.

Although DMCT appears stable in ether-based electrolytes, the conversion reaction is limited to a 2-electron transfer. This limits the theoretical energy density to ~ 941 Wh kg^{-1}. To overcome this limit, Inoue *et. al.* synthesized polyDMCT-tetrasulfide, which can undergo a 6-electron reaction due to the presence of 2 additional sulfur atoms to possess a theoretical specific capacity of 758.5 mA h g^{-1}, which increases the energy density to 1710 Wh kg^{-1}. Unfortunately, in this report, the authors used a carbonate-based electrolyte and thus observed no reversible redox reactions. Therefore, they relegated polyDMCT-tetrasulfide as a non-rechargeable/primary battery material.

In this work, we revisit pDMCT-based materials armed with the knowledge of electrolytes that are stable with both sulfur/organosulfur materials as well as alkali-metal anodes. We synthesize pDMCT with 2 additional sulfurs – pDMCT-S through a facile condensation reaction between DMCT and sulfur. Cells with pDMCT-S cathode and Li-metal anode demonstrate a reversible capacity of 611 mA h g^{-1} when cycled at a C/2 rate. This high material utilization placates concerns about the non-rechargeability and sluggish kinetics previously associated with pDMCT-based materials. Surprisingly, it was found that the cycling stability of the pDMCT-S cathode was better than that of a sulfur cathode. Further investigation into the source of this stability revealed the ability of the discharged product of pDMCT-S to interact with and bind to polysulfides. This unique interaction significantly reduces the polysulfide "shuttle" effect that is known to plague elemental sulfur cathodes. Cells with Na-metal anode were also fabricated. A dramatic improvement in the performance of Na||pDMCT-S against a sulfur cathode highlights the effectiveness of such materials as inherent polysulfide regulators, which have so far been unexplored.

2. Results and Discussion

2.1. Synthesis and Characterization of pDMCT-S

The tetrasulfide polymer of DMCT *i.e.,* poly[tetrathio-2,5-(1,3,4-thiadiazole)] or pDMCT-S, was chosen for this study as it offers the following benefits: (i) thiols can be easily oxidized to polysulfide polymers through a host of synthetic routes;[17,26–28] (ii) the additional sulfur in the polysulfide polymer enhances the capacity of DMCT-based polymers and therefore the achievable energy density; (iii) the thiadiazole ring withdraws electrons from the sulfur in the thiol group, thus increasing its redox potential compared to neutral sulfur and improving the energy density;[29,30] and iv) constraining the polysulfide chain in the polymer to a tetrasulfide curbs the formation of electrolyte-soluble higher-order polysulfides that cause the shuttle effect.[31]

pDMCT-S was synthesized with a base-catalyzed reaction between thiols and elemental sulfur.[32] This technique was chosen as it can be performed at room temperature without the need for an inert atmosphere and because the product is obtained in the solution form that can be used without further purification. In a typical synthesis, 1 equivalent of DMCT and 3 equivalents of sulfur were dissolved in a 1:1 v/v mixture of 1,3 dioxolane (DOL) and carbon disulfide (CS_2). The complete dissolution of both precursors in the solvents ensures a homogenous and complete reaction. The addition of 10 – 15 μL of ethylenediamine was sufficient to initiate and catalyze the reaction as shown in **Figure 1a**. The reaction proceeded with the rapid evolution of H_2S gas which subsided within 30 min to signal the completion of the reaction. The resulting, yellow-colored solution was either drop cast onto commercial carbon nanotube (CNT) paper discs, followed by drying to yield the cathodes, or was dried to remove the solvents to obtain the polymer for materials characterization. The scanning electron microscope (SEM) image along with the inset energy-dispersive x-ray (EDX) analysis of the cathode in Figure 1a shows that the polymer is uniformly deposited as nodules of 500 nm to 1 μm diameter within the CNT network. The highly conductive and porous network of the CNTs can sufficiently accommodate the polymer while also providing abundant electron- and ion-conducting channels for efficient material utilization.

A suite of materials characterization was applied to confirm the completion of the synthesis reaction and to understand the nature of the polymer. The x-ray diffraction (XRD) study in **Figure 1b** shows that the precursors namely DMCT and sulfur are highly crystalline. In contrast, pDMCT-S shows no characteristic peaks except a broad feature at low 2θ up to 35°, indicating its amorphous nature. ^{1}H-nuclear magnetic resonance study in **Figure 2c** shows that the characteristic peak of the proton from the thiol in DMCT at 13.23 ppm is absent on polymerization to pDMCT-S. The NMR data, along with the XRD and Fourier transform infrared (FTIR) spectroscopy data in **Figure S1**, confirm the complete conversion of DMCT to pDMCT-S.

X-ray photoelectron spectroscopy (XPS) was employed to understand the degree of sulfur incorporated into DMCT. The S 2p region scans of DMCT and pDMCT-S in **Figure 2d** highlight two major observations. First, the peak with S $2p_{3/2}$ at 162.13 eV corresponding to the thiol bond in DMCT disappears. Also, the S $2p_{3/2}$ peak at 164.4 eV in DMCT corresponding to the sulfur in the thiadiazole ring in DMCT undergoes a significant negative shift to 162.6 eV in pDMCT-S, owing to the loss of resonance in the thiadiazole ring. This confirms the oxidation of the thiol when converting DMCT to pDMCT-S.[33] Second, the peak at 164.9 eV in pDMCT-S indicates the presence of neutral sulfur. Furthermore, the area ratio between the neutral sulfur and the heterocyclic sulfur is about 4 : 1, thus indicating the formation of a tetrasulfide polymer.

2.2. Electrochemical Response and Reaction Mechanism in Li-metal Batteries

In theory, the synthesized tetrasulfide polymer should undergo a 6-electron reaction yielding a specific capacity of 758 mA h g^{-1} and a specific energy of 1710 Wh kg^{-1}. The electrochemical response of the pDMCT-S cathode was studied with Li-metal foil as the counter and reference electrode. 2032-type cells were fabricated with pDMCT-S/DMCT cathodes having a loading of 2.2 mg cm^{-2}. The electrolyte commonly used with sulfur cathodes was used: 1 M lithium bis(trifluoromethanesulfonyl)imide (LiTFSI) in 1,2-dimethoxyethane (DME) and 1,3-dioxolane (DOL) (1:1 v/v) with a 0.2 M lithium nitrate ($LiNO_3$) additive to passivate the Li-metal anode.[5]

These cells were galvanostatically cycled at a C/10 rate and the representative voltage profile is shown in **Figure 2a**. The complementary technique of cyclic voltammetry (CV) was performed at a scan rate of 0.05 mV s^{-1} as shown in **Figure 2b**. As can be seen, the discharge-charge process occurs in 4 steps, each at a distinct voltage. The open-circuit voltage (OCV) of pDMCT-S is about 3.05 V. As the cell is discharged, the first plateau (I) occurs at 2.91 V and contributes 82 mA h g^{-1}. The bond dissociation enthalpy and consequently the Gibbs free energy change for the cleavage of the C-S-S bond (indicated in the scheme shown in **Figure 2c**) is higher than that of neutral S-S bonds due to the electron-withdrawing nature of the thiadiazole ring.[34] This explains the high voltage for this initial discharge reaction. The discharge product from this step undergoes further reduction at the C-S-S linkage as shown in the scheme at 2.63 V, which is indicated as plateau II in the voltage profile. This step offers 95 mA h g^{-1}. It is interesting to note that pure DMCT also undergoes a similar 2-step reduction process, thus confirming that the sulfur atoms bonded closest to the ring in the polymer are the most labile for cleavage. At the end of the second discharge step, lithiated DMCT (Li-DMCT) along with Li_2S_2 is generated. The Li_2S_2 can undergo disproportionation to lithium polysulfides which undergo further reduction to Li_2S through plateaus III and IV at, respectively, 2.37 and 2.05 V. This transformation resembles that of sulfur cathodes. Overall, the pDMCT-S delivers a capacity of 715 mA h g^{-1}, suggesting that the depolymerization reaction is facile. It is also worth noting that Li-DMCT can exist in its mesomeric form as shown in Figure 2c. This mesomeric stabilization of Li-DMCT would also explain why the bonds that lead to its formation break first. Additional benefits of this mesomer will be discussed in later sections.

During charge, the process is reversed with the formation of polysulfides in steps V and VI. Steps VII and VIII involve the reconstruction of the pDMCT-S polymer. The similarity between the potentials for the reconstruction of DMCT and pDMCT-S indicate that the delithiation of Li-DMCT occurs after polysulfide formation, thus resulting in an effective reincorporation of sulfur into the polymer. The CV data points to 4 peaks corresponding to voltage plateaus VII and VII. This suggests that the mesomeric form of Li-DMCT could play a role in guiding the reformation of the polymer. The overall charge capacity is 732 mA h g^{-1}, equating to a Coulombic efficiency (CE) of 97.7 %, which indicates that the polymer can be reformed without significant deviation in the mechanism.

In order to validate the proposed discharge-charge mechanism, XPS was performed on the cathodes in the pristine, fully discharged, and fully charged state as shown in **Figure 2d**. The S 2p XPS data of the discharged cathode shows a clear $2p_{3/2}$ peak at 160 eV, confirming the formation of Li_2S from the neutral sulfurs in the polymer. The peak at 161.8 eV is similar to that of the thiol peak in DMCT. This confirms the formation of Li-DMCT. This is further confirmed by the peak for the sulfur in the thiadiazole ring at 163.8 eV akin to DMCT. XRD analysis of the discharged cathode (**Figure S2a**) suggests that the Li-DMCT is crystalline while the Li_2S is amorphous. Upon charge, the peak corresponding to neutral sulfur at 164.8

eV is observed, confirming the reformation of the polysulfide polymer. No residual peaks of Li-DMCT are observed, which agrees with the good reversibility observed in the voltage and CV data. Additionally, the ratio of peak areas between the S-S bond and the C-S-C bond is about 4 : 1, indicating that the sulfur is successfully reintegrated into the polymer. This area ratio is maintained even after Ar^+ sputtering, suggesting a uniform distribution of sulfur within the polymer (**Figure S3**) through the depth of the electrode. The successful reformation of the polymer on recharge is corroborated by the XRD analysis of the cathode (**Figure S2b**).

To computationally validate this reaction mechanism, the lowest unoccupied molecular orbital (LUMO) and the highest occupied molecular orbital (HOMO) energy levels of the reaction intermediates were calculated through first-principles density functional theory (DFT), as depicted in **Figure 2e**. An oligomer of three repeating pDMCT-S units was used to approximate the polymer. This structure has a LUMO of -2.91 eV and a HOMO of -5.50 eV. The lithiated intermediate expected in the plateaus I and VIII, as indicated in the scheme in Figure 2c, has a LUMO of -2.02 eV and a HOMO of -5.45 eV. This increase in enegy levels suggets that such a structure is a viable intermediate and would occur at a lower voltage than pDMCT-S. The significant increase in the energy levels in Li-DMCT, which is expected to be formed in plateaus II and VII (LUMO: -0.78 eV and HOMO: -5.21 eV), points to a wide potetial difference between the pDMCT-S and Li-DMCT states, which is in agreement with the voltage profiles. These DFT results corroborate the stepwise lithiation of pDMCT-S.

2.3. Performance and Origins of Stability

After confirming its rechargeability, the long-term stability of pDMCT-S as a cathode material was tested through galvanostatic cycling. Sulfur cathodes with identical parameters as pDMCT-S cathodes were also tested to assess the benefits of using pDMCT-S as an active material. **Figure 3a** shows the cyclability of the cathodes when cycled at a C/2 rate with the capacity of pDMCT-S being normalized on a sulfur basis for a fair comparison. pDMCT-S yields a first cycle discharge capacity of 611 mA h g^{-1} corresponding to 1018 mA h g^{-1} on a sulfur basis. This is comparable to the sulfur cathode that yields 980 mA h g^{-1}. Both cells show relative stability until 50 cycles. Beyond this point, a rapid decline in the capacity of sulfur is observed with only about 50 % of the initial capacity retained after 100 cycles. In sharp contrast, pDMCT-S shows a gradual decline in capacity and retains 83.5 % of its initial capacity after 100 cycles. This stark contrast is also seen in the CE between the cells. pDMCT-S can maintain a high average CE of 99.2 % while sulfur cathode can sustain only 96.3 %. The higher CE of pDMCT-S cathodes indicates lowered polysulfide shuttle effect suggesting a better encapsulation of the polysulfides within the polymer compared to the sulfur cathode. Representative voltage profiles from these cells (**Figure 3b**) show that the increased current density does not dramatically lower the operating potential of pDMCT compared with that of low-current-density cycling (Figure 2a). Consequently, the average difference between the discharge and charge voltages for pDMCT is only 270 mV. Meanwhile, this difference is as high as 524 mV for the sulfur cathode. This suggests that the rapid depolymerization and repolymerization reactions that occur during the operation of the pDMCT-S cathode are not kinetically sluggish. In fact, pDMCT-S redox appears to be even better than that of sulfur redox. Examination of the evolution of the voltage with cycling (**Figure S4**) highlights that the ratio of capacities delivered at each voltage does not vary. This indicates the high reversibility of the discharge/charge reactions. pDMCT-S cathode was also cycled at various rates (**Figure S5**). The ability to consistently deliver high capacities including about 580 mA h g^{-1} on a pDMCT-S basis or 967 mA h g^{-1} on a sulfur basis at a 1C rate sufficiently placates the previously reported concerns about the sluggishness of the reactions when using DMCT-based polymers.

These surprising results, including the ability to outperform sulfur cathodes, prompted the investigation into the origin of this stability. It was suspected that the ability of Li-DMCT to exist in the mesomeric form was aiding in the stability of the pDMCT-S cathode. Probing the N 1s XPS spectra of the pDMCT-S cathode at different stages of cycling (**Figure 3c**) reveals a negative shift in the peak corresponding to the nitrogen in the thiadiazole ring from 401.2 eV in the pristine polymer to 399.4 eV in the discharged state. This shift is absent in the recharged polymer. This signifies that the coexistence of Li-DMCT and Li_2S in the discharged state helps stabilize the mesomeric form. Subsequently, the polymer powder was added to a 50 mM solution of lithium polysulfide in DOL to observe their interaction. As seen in the photograph in **Figure 3d**, the deep red polysulfide solution turns yellow while a yellowish-white precipitate settles at the bottom of the vial within 2 h. Analysis of the solution through ultraviolet-visible (UV-Vis) spectroscopy (**Figure 3e**) confirms the strong binding of the polysulfide to the polymer through the disappearance of characteristic polysulfide peaks at 300 and 420 nm.[35] It was also confirmed that the final yellow color of the solution originates from the dissolved pDMCT-S remaining in the solution (**Figure S6**).[33] FTIR spectroscopy was performed on the precipitate formed by the interaction between lithium polysulfide and pDMCT-S (**Figure S7**). Analysis of the spectra in the 1600 – 1000 cm^{-1} region shows that the peaks corresponding to C=N and N-N vibrations are shifted to lower frequency, indicating a strong interaction between the thiadiazole ring and polysulfide anion via the lithium bonded to the nitrogen centers.[36] Additionally, XRD study of the precipitate formed (**Figure S8**) shows peaks similar to Li-DMCT albeit with a slight shift and no obvious peaks of elemental sulfur. This confirms the strong confinement of polysulfide within the crystals of Li-DMCT. The interaction between lithium polysulfide and Li-DMCT was studied through an absorption test. As shown in **Figure S9**, the deep-red color of the polysulfides dissipated and a yellow solution was obtained along with yellow-white precipitates. This result is analogous to the pDMCT-S – polysulfide absorption test. This suggests that the thiadiazole center is the key to polysulfide absorption.

To supplement the experimental evidence, *ab-initio* molecular dynamics (AIMD) calculations were performed to understand the interaction between the mesomeric form of DMCT, which is analogous to Li-DMCT, and lithium polysulfides. The equilibrium molecular structure obtained after the interaction of DMCT with Li_2S_4 as a representative polysulfide is shown in **Figure 3f**. The average partial charge on the nitrogen in the thiadiazole ring is indicated below the structures. The relaxed structure shows that the lithium from the polysulfide is shared with DMCT through the thiol-type sulfur and the nitrogen centers. The reduction in the partial charge of nitrogen centers indicates the Li-ion mediated stabilization of the mesomer, which is consistent with XPS and UV-Vis results. Each Li-DMCT can potentially bind with two lithium polysulfide molecules rendering these clusters bulky and hence less soluble in the electrolyte, resulting in their precipitation as seen in Figure 3d. This phenomenon explains the reduced polysulfide shuttle effect and consequently, the improved cycling stability observed in the pDMCT-S cathode. While these equilibrium structures confirm the sites of interaction, it is, however, important to note that they might represent local minima in terms of the energy of interaction. The degree of interaction would be affected by concentration, temperature, and the solvating power of the electrolyte solvents. Interestingly, these structures indicate that Li-DMCT would promote Li-ion conductivity and facilitate charge transfer into the lithium polysulfides. This was verified through the electrochemical impedance spectroscopy (EIS) data in **Figure S10**. The lowering of charge-transfer resistance in the pDMCT-S cathode when compared to the sulfur cathode corroborates the facile ion- and electron-transport through pDMCT-S. The effects of this mediation of discharge and charge by Li-DMCT can be seen in the SEM images in **Figure S11,** which show the uniform deposition of discharge and charge products on cycling. As a result of the strong interactions and redox mediation, the pDMCT-S cathode can operate with low overpotentials and high utilization of sulfur. This unique capability of thiadiazole highlights that the use of similar organic functional groups can preclude the use of inorganic electrocatalytic hosts to enhance performance in metal-sulfur batteries. In addition to the benefits at the cathode, the polysulfide encapsulation by pDMCT-S also helps the Li-metal anode. The SEM images in **Figure S12** compare the morphology of the Li-metal surface on cycling with a sulfur cathode against a pDMCT-S cathode. The unregulated polysulfide shuttle from the sulfur cathode results in mossy and dendritic Li deposits. On the other hand, with the pDMCT-S cathode, the reduction in polysulfide migration results in smoother Li deposits.

The benefits of using pDMCT-S prompted the testing of the cathodes under practically relevant high-loading and lean-electrolyte scenarios.[37] Cathodes with a pDMCT-S loading of 4.4, 5.5, and 6.6 mg cm^{-2} were tested at a C/10 rate with an electrolyte load of 7 µL mg^{-1} on a pDMCT-S basis. The performance in **Figure S13** shows that the cathodes with 4.4, 5.5, and 6.6 mg cm^{-2} loading can deliver, respectively, 1009, 873, and 748 mA h g^{-1} on a sulfur basis. This high utilization of sulfur reaffirms the benefits of Li-DMCT mediated redox. Furthermore, the cells with a loading of 4.4, 5.5, and 6.6 mg cm^{-2} retained, respectively, 79 %, 72 %, and 70 % of their initial capacity, indicating the successful mitigation of polysulfide shuttle effect by pDMCT-S even at high loadings. These encouraging results show that pDMCT-S has the potential for practical applications.

2.4. Electrochemical Response and Performance in Na-metal Batteries

Sodium is seen as a sustainable alternative to Li-metal anode due to its high abundance. However, sodium-sulfur battery technology is less mature than lithium-sulfur technology due to the following intrinsic chemistry challenges: (i) Due to the larger size of Na^+ compared to Li^+, its conduction through precipitated sodium polysulfides (particularly Na_2S_4) and its subsequent conversion reaction to form Na_2S is kinetically sluggish resulting in low capacity.[38,39] (ii) Sodium polysulfides are extremely soluble compared to their lithium counterparts in the commonly used tetraethyleneglycol dimethylether (TEGDME)-based electrolyte, leading to rapid sulfur loss from the cathode and therefore capacity decay.[25] (iii)

The Na-metal passivation provided by the sodium nitrate ($NaNO_3$) additive is lower than that of $LiNO_3$ for Li-metal anodes. This aggravates the polysulfide shuttle effect and results in poor CE.

Encouraged by the capability of pDMCT to promote sulfur redox and internally sequester polysulfides, Na-anode cells were fabricated with a 1 M sodium perchlorate ($NaClO_4$) in TEGDME with 0.2 M $NaNO_3$ additive to promote anode passivation. **Figure 4a** shows the voltage profile on galvanostatic cycling of pDMCT at C/10 rate and **Figure 4b** shows the CV scan performed at 0.05 mV s^{-1}. As with Li-metal anode cells, the Na-metal anode cells show distinct 4-step discharge/charge mechanism. The OCV is 2.92 V and on discharging, the first plateau (I) occurs at 2.81 V while contributing 80 mA h g^{-1}. This plateau is only 100 mV lower and yields nearly identical capacity as with the Li-anode. The closeness of discharge voltage and capacity across systems indicates that this reaction step is facile in ether-based electrolytes. The second plateau labeled II occurs at 2.4 V and contributes 82 mA h g^{-1}. The 230 mV difference when compared with Li-anode accentuates the resistace typically offered by sulfur towards sodiation. Despite this, a capacity comparable with Li-anode system is obtained, signifying that the overall electronic and Na-ion conduction facilitated by pDMCT-S and the electrode design is vital to overcome this resistance. Following this, pDMCT discharges through plateaus III and IV at, respectively, 2.27 and 1.66 V, which is typical of polysulfide redox. A reasonable capacity of 410 mA h g^{-1} can be extracted overall corresponding to the utilization of 54 % of the active material. During charge, similar to the mechanism in the Li-based cells, the redox process is reversed and with a charge capacity of 426 mA h g^{-1}. The high initial CE of 96.2% emphasizes the ability of pDMCT-S to repolymerize without much shuttling or loss of sulfur.

The long-term cyclability of pDMCT and a sulfur cathode was compared at C/10 as shown in **Figure 4c**. 410 mA h g^{-1} can be extracted from pDMCT-S, which corresponds to 683 mA h g^{-1} on a sulfur basis. Sulfur, on the other hand, can yield only 415 mA h g^{-1}.

Additionally, pDMCT displays an average CE of 97.2 %, whereas sulfur can only maintain an average CE of 81 %. This confirms that the unchecked polysulfide shuttle in the case of the sulfur cathode is the main source of capacity fade, which is why only 10 % of the initial capacity can be retained after 50 cycles. Similar to Li-based cells, the Na-DMCT can strongly bind to sodium polysulfides during charge and encapsulate the polysulfide within the pDMCT-S upon repolymerization. Consequently, the shuttle effect is significantly reduced, leading to an improved capacity retention of 65.8 %.

The voltage profiles of the pDMCT-S and sulfur cathodes displayed in **Figure S14** were scrutinized to understand the difference in the kinetics between the electrodes. The difference in average potential between the charge and discharge for the sulfur cathode is 408 mV, while it was only 236 mV for the pDMCT-S cathode. This substantiates that polysulfide binding by Na-DMCT, improved electronic conductivity through electron delocalization in the thiadiazole ring, and ionic conductivity provided by Na-ions bound to the nitrogen center can boost the kinetics by mediating sulfur redox within the pDMCT-S cathode. Apart from improving the capacity, the average discharge voltage is increased to 2.15 V in pDMCT-S from 1.8 V in the sulfur cathode. This means that the material level specific energy is improved from 747 Wh kg^{-1} for sulfur to 880 Wh kg^{-1} for pDMCT-S.

3 Conclusion

A reconsideration of pDMCT-based cathodes in the form of pDMCT-S, while using appropriate electrolyte and cathode design, demonstrates its excellent rechargeability in both Li- and Na-metal anode batteries. It was found that pDMCT-S can undergo reversible redox through a 4-step discharge/charge process. The mesomeric form of the discharge product Li/Na-DMCT was shown to absorb polysulfide through strong binding at the nitrogen centers of the thiadiazole ring. This minimizes the polysulfide shuttle and promotes sulfur redox. Consequently, improved cycling stability is observed with pDMCT-S cathodes compared to sulfur cathodes in both Li- and Na-metal anode cells. The versatility of the thiadiazole functional group in pDMCT-S highlights the opportunity to design other multi-functional organosulfur materials that can also regulate the polysulfide shuttle effect. Alternatively, such organosulfur materials can be used as additives in conventional sulfur cells to tame the polysulfides. This strategy provides an alternative to the current reliance on inorganic metal-based materials, such as transition-metal chalcogenides, to prevent shuttle and improve the kinetics of sulfur redox. We hope that this work will encourage the exploration of such multi-functional organosulfur materials that can enable long-life, high-energy metal-sulfur batteries.

4. Experimental Section

Materials:

All reagents were purchased from Sigma-Aldrich or Acros Organics and used as received. Commercial CNT "buckypaper" (20 GSM) was purchased from NanoTechLabs, Inc.

pDMCT-S synthesis:

In a typical synthesis, 3 eq. of elemental sulfur (usually 96 mg) was completely dissolved in a vial containing 2 mL of a 1:1 v/v mixture of dissolved-oxygen-free DOL/CS_2 solvents. 1 eq. of DMCT (usually 150.2 mg) was then dissolved into this solution. The addition of about 10 – 15 µL of ethylene diamine led to effervescence, which faded after 30 min. The solution was stirred for an additional hour to yield a 0.5 M pDMCT-S solution.

Fabrication of pDMCT-S and sulfur cathodes:

CNT paper was mildly calendared, punched into 7/16-inch discs (each roughly weighing 1.9 mg cm^{-2}), and dried in a vacuum at 100°C overnight. An appropriate amount of either the polymer solution (as synthesized above) or a 0.5 M solution of elemental sulfur in CS_2 was drop cast on dried CNT paper discs placed in a teflon petri-dish. The drop cast electrodes were dried in air for 1 h, followed by drying at 60°C for 12 h under vacuum. A typical cathode was loaded with 2.2 mg cm^{-2} of active material. For high loading cathodes, the steps outlined above were repeated until the desired loading was achieved.

Li-DMCT synthesis:

All operations were performed inside an Ar-filled glovebox. DMCT was first dissolved in tetrahydrofuran (THF) to form a 1 M solution. To this, 1.0 M lithium triethylborohydride in THF was slowly added in the appropriate stoichiometry to yield Li-DMCT. The THF was then removed under vacuum. The resulting white powder was recrystallized with THF before use.

Coin-cell fabrication and electrochemical testing:

Standard CR-2032-type coin cells were assembled inside an Ar-filled glovebox for all cases. For Li-metal cells, the cathode was paired with an electrolyte consisting of 1 M LiTFSI in a 1 : 1 v/v mixture of DME and DOL with a 0.2 M $LiNO_3$ additive, a celgard 2500 separator, and a Li-metal foil anode attached to a Ni-foam spacer. For Na-metal cells, the cathode was paired with an electrolyte consisting of 1 M $NaClO_4$ in TEGDME with a 0.2 M $NaNO_3$ additive, a celgard 2500 separator, and a Na-metal foil anode. The electrolyte to active material ratio was usually 15 μL mg^{-1} unless otherwise noted.

Galvanostatic cycling was performed on Arbin cyclers at an appropriate current density. A current density of 1C = 758 mA g^{-1} was used for pDMCT-S cathodes and that of 1C = 1672 mA g^{-1} was used for sulfur cathodes. The current density was based on the active material loading in the cathode. Li-metal cells were cycled between 1.8 and 3.3 V, while Na-metal cells were cycled between 1.2 and 3 V. CV was performed on a BioLogic VSP potentiostat at a scan rate of 50 μV s^{-1} between the same voltage ranges as galvanostatic cycling. EIS was performed from 1 MHz to 0.1 Hz on cells rested at OCV for 2 h.

Polysulfide absorption test:

50 mM of lithium polysulfide (Li_2S_6) solution was prepared by stirring an appropriate amount of Li_2S and S overnight. Into 4 mL of this solution, 100 mg of pDMCT-S was added and stirred for 5 min. The solution was then left to stand undisturbed for 2 h before acquiring the photograph. Similar procedure was followed for the Li-DMCT - Li_2S_6 absorption test while using 80 mg of Li-DMCT.

Materials characterization:

SEM micrographs were obtained on a FEI Quanta 650 SEM operated at 10 kV and EDX mapping was performed on the attached Bruker detector. XRD was performed on a Bruker MiniFlex 600 X-ray diffractometer with Cu Kα radiation and $2\theta = 20°$ to 60°. NMR was performed on a Bruker Avance III 500 MHz NMR spectrometer. A mixture of DOL and $CDCl_3$ was used to dissolve the samples. Solvent peaks were used to calibrate the chemical shifts. XPS data were acquired with a Kratos AXIS Ultra DLD spectrometer with monochromatic Al Kα radiation. Data were analyzed using the CASA XPS software. The adventitious carbon peak at 284.8 eV was used to calibrate the spectra. Shirley background was used and Gaussian/Lorentzian peaks were fitted in the S 2p region. FTIR studies were performed on a Thermo Scientific-Nicolet iS5 spectrometer. Samples were infused into KBr pellets for measurement. 64 scans were acquired in the 400 to 4000 cm^{-1} region. UV-Vis spectroscopy was performed on Cary 5000 UV-VIS NIR Spectrometer with samples that were diluted 10-fold in DOL and characterized in a wavelength range of 220 to 800 nm.

AIMD Calculations:

The relaxed structures were obtained using the Vienna *ab initio* simulation package (VASP).[40,41] Generalized gradient approximation (GGA) with Perdew-Burke-Ernzerhof PBEexchange-correlation functional was used, in conjunction with the projector augmented wave (PAW) pseudopotentials.[42,43] The initial geometry of the Li_2S_4-attached DMCT was manually generated. An energy cutoff of 600 eV with a Monhrost-Pack reciprocal space grid of 1 x 1 x 1 *k*-points scheme was used.[44] Once the structures are relaxed, a Bader-charge analysis was conducted to obtain the partial charge of atoms.[45] Calculations of the HOMO/LUMO energy levels were performed with the use of Gaussian 09 Rev. A.02. The B3LYP method along with the Pople basis set 6-31+G(d,p) was used. The input geometrical structures were obtained by relaxing the manually generated structures in VASP. An oligomer with three repeating units of pDMCT-S was used to approximate the polymer structure. An implicit solvation through polarizable continuum model (PCM) with THF as the solvent was used.

Supporting Information
Supporting Information is available from the Wiley Online Library or from the author.

Acknowledgments

This work was supported by the U.S. Department of Energy, Office of Basic Energy Sciences, Division of Materials Science and Engineering under award number DE-SC0005397. The authors would like to thank Dr. Anil Parameswaran Thankam for assistance in polymer synthesis and Dr. Woochul Shin for assistance in performing theoretical calculations.

Received: (will be filled in by the editorial staff)
Revised: (will be filled in by the editorial staff)
Published online: (will be filled in by the editorial staff)

References

[1] A. Manthiram, *Nat. Commun.* **2020**, *11*, 1550.

[2] W. Li, E. M. Erickson, A. Manthiram, *Nat. Energy* **2020**, *5*, 26.

[3] Y. Zhou, D. Gohlke, L. Rush, J. Kelly, Q. Dai, **2021**, DOI 10.2172/1778934.

[4] S. S. Sharma, A. Manthiram, *Energy Environ. Sci.* **2020**, *13*, 4087.

[5] S. Chung, A. Manthiram, *Adv. Mater.* **2019**, *31*, 1901125.

[6] D. Y. Wang, W. Guo, Y. Fu, *Acc. Chem. Res.* **2019**, *52*, 2290.

[7] W. Guo, D. Y. Wang, Q. Chen, Y. Fu, *Adv. Sci.* **2022**, *9*, 2103989.

[8] Z. Shadike, S. Tan, Q. C. Wang, R. Lin, E. Hu, D. Qu, X. Q. Yang, *Mater. Horizons*

2021, *8*, 471.

[9] Y. Chen, S. Zhuo, Z. Li, C. Wang, *EnergyChem* **2020**, 100030.

[10] H. Lyu, X.-G. Sun, S. Dai, *Adv. Energy Sustain. Res.* **2021**, *2*, 2000044.

[11] S. J. Visco, *J. Electrochem. Soc.* **1988**, *135*, 2905.

[12] M. Liu, S. J. Visco, L. C. De Jonghe, *J. Electrochem. Soc.* **1989**, *136*, 2570.

[13] S. J. Visco, M. Liu, L. C. De Jonghe, *J. Electrochem. Soc.* **1990**, *137*, 1191.

[14] M. Liu, S. J. Visco, L. C. De Jonghe, *J. Electrochem. Soc.* **1991**, *138*, 1891.

[15] P. Novák, K. Müller, K. S. V Santhanam, O. Haas, *Chem. Rev.* **1997**, *97*, 207.

[16] N. Oyama, T. Tatsuma, T. Sato, T. Sotomura, *Nat. 1995 3736515* **1995**, *373*, 598.

[17] K. Naoi, K. Kawase, Y. Inoue, *J. Electrochem. Soc.* **1997**, *144*, L170.

[18] N. Oyama, Y. Kiya, O. Hatozaki, S. Morioka, H. D. Abruña, *Electrochem. Solid-State Lett.* **2003**, *6*, A286.

[19] Y. Kiya, A. Iwata, T. Sarukawa, J. C. Henderson, H. D. Abruña, *J. Power Sources* **2007**, *173*, 522.

[20] J. Gao, M. A. Lowe, S. Conte, S. E. Burkhardt, H. D. Abruña, *Chem. – A Eur. J.* **2012**, *18*, 8521.

[21] S. C. Canobre, R. A. Davoglio, S. R. Biaggio, R. C. Rocha-Filho, N. Bocchi, *J. Power Sources* **2006**, *154*, 281.

[22] L. Jin, G. Wang, X. Li, L. Li, *J. Appl. Electrochem.* **2011**, *41*, 377.

[23] T. Yim, M. S. Park, J. S. Yu, K. Kim, K. Y. Im, J. H. Kim, G. Jeong, Y. N. Jo, S. G. Woo, K. S. Kang, I. Lee, Y. J. Kim, *Electrochim. Acta* **2013**, *107*, 454.

[24] Y. Zhang, Y. Zhong, Q. Shi, S. Liang, H. Wang, *J. Phys. Chem. C* **2018**, *122*, 21462.

[25] J. He, A. Bhargav, W. Shin, A. Manthiram, *J. Am. Chem. Soc.* **2021**, *143*, 20241.

[26] Y. Zhang, R. S. Glass, K. Char, J. Pyun, *Polym. Chem.* **2019**, *10*, 4078.

[27] A. Bhargav, M. E. Bell, J. Karty, Y. Cui, Y. Fu, *ACS Appl. Mater. Interfaces* **2018**, *10*, 21084.

[28] A. Bhargav, M. E. Bell, Y. Cui, Y. Fu, *ACS Appl. Energy Mater.* **2018**, *1*, 5859.

[29] W. Guo, Z. Wawrzyniakowski, M. Cerda, A. Bhargav, M. Pluth, Y. Ma, Y. Fu, *Chem. – A Eur. J.* **2017**, *23*, 16941.

[30] A. Bhargav, A. Manthiram, *Adv. Energy Mater.* **2020**, *10*, 2001658.

[31] A. Bhargav, C. H. Chang, Y. Fu, A. Manthiram, *ACS Appl. Mater. Interfaces* **2019**, *11*, 6136.

[32] B. K. Bordoloi, E. M. Pearce, *J. Appl. Polym. Sci.* **1979**, *23*, 2757.

[33] C. Li, S. Huang, C. Min, P. Du, Y. Xia, C. Yang, Q. Huang, *Polym. 2018, Vol. 10, Page 24* **2017**, *10*, 24.

[34] L. F. Zou, Y. Fu, K. Shen, Q. X. Guo, *J. Mol. Struct. THEOCHEM* **2007**, *807*, 87.

[35] A. Gupta, A. Bhargav, A. Manthiram, *Adv. Energy Mater.* **2018**, *0*, 1803096.

[36] J. M. Pope, T. Sato, E. Shoji, N. Oyama, K. C. White, D. A. Buttry, *J. Electrochem. Soc.* **2002**, *149*, A939.

[37] A. Bhargav, J. He, A. Gupta, A. Manthiram, *Joule* **2020**, *4*, 285.

[38] A. Manthiram, X. Yu, *Small* **2015**, *11*, 2108.

[39] X. Yu, A. Manthiram, *Adv. Funct. Mater.* **2020**, *30*, 2004084.

[40] G. Kresse, J. Hafner, *Phys. Rev. B* **1993**, *47*, 558.

[41] G. Kresse, J. Hafner, *Phys. Rev. B* **1994**, *49*, 14251.

[42] J. P. Perdew, K. Burke, M. Ernzerhof, *Phys. Rev. Lett.* **1996**, *77*, 3865.

[43] P. E. Blöchl, *Phys. Rev. B* **1994**, *50*, 17953.

[44] H. J. Monkhorst, J. D. Pack, *Phys. Rev. B* **1976**, *13*, 5188.

[45] G. Henkelman, A. Arnaldsson, H. Jónsson, *Comput. Mater. Sci.* **2006**, *36*, 354.

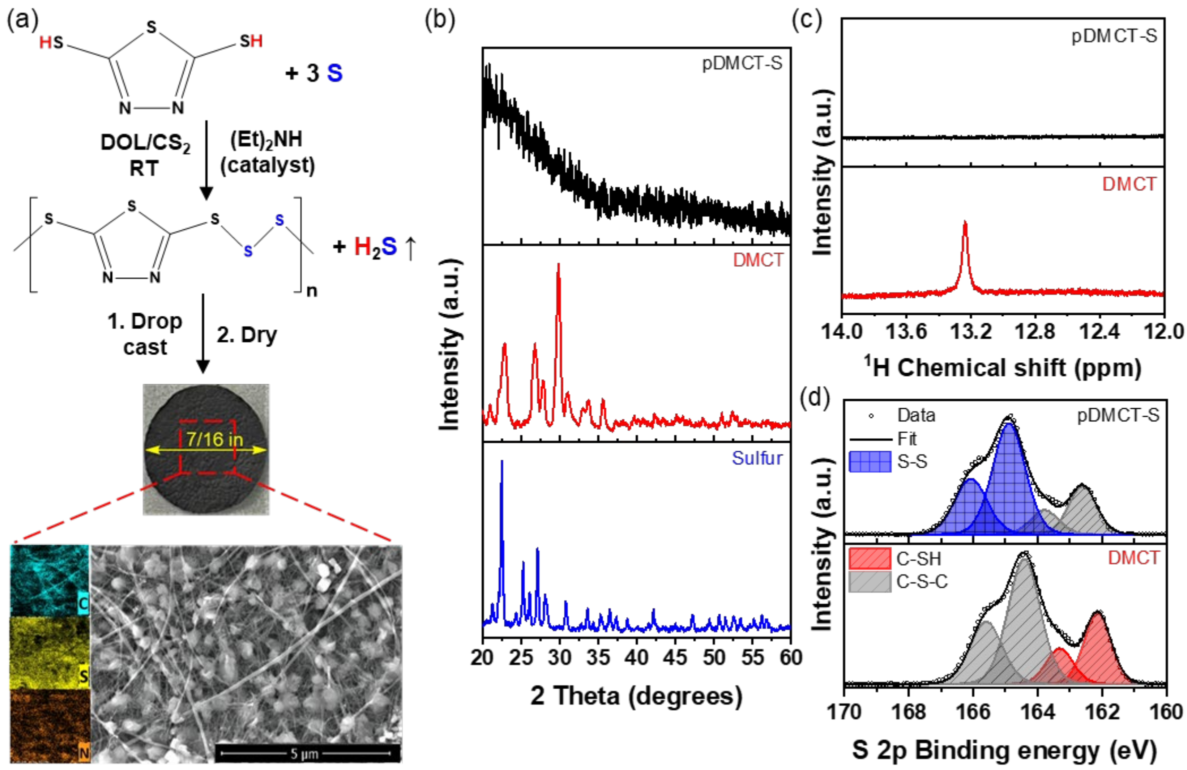

Figure 1. (a) Reaction scheme showing the synthesis of pDMCT-S and the cathode preparation procedure. The attached SEM image shows the microstructure of the cathode and the EDX mapping highlights the distribution of elements. (b) XRD of the precursors and the synthesized pDMCT-S. (c) ^{1}H-NMR of DMCT and pDMCT-S. (d) S 2p XPS region scans of DMCT and pDMCT-S.

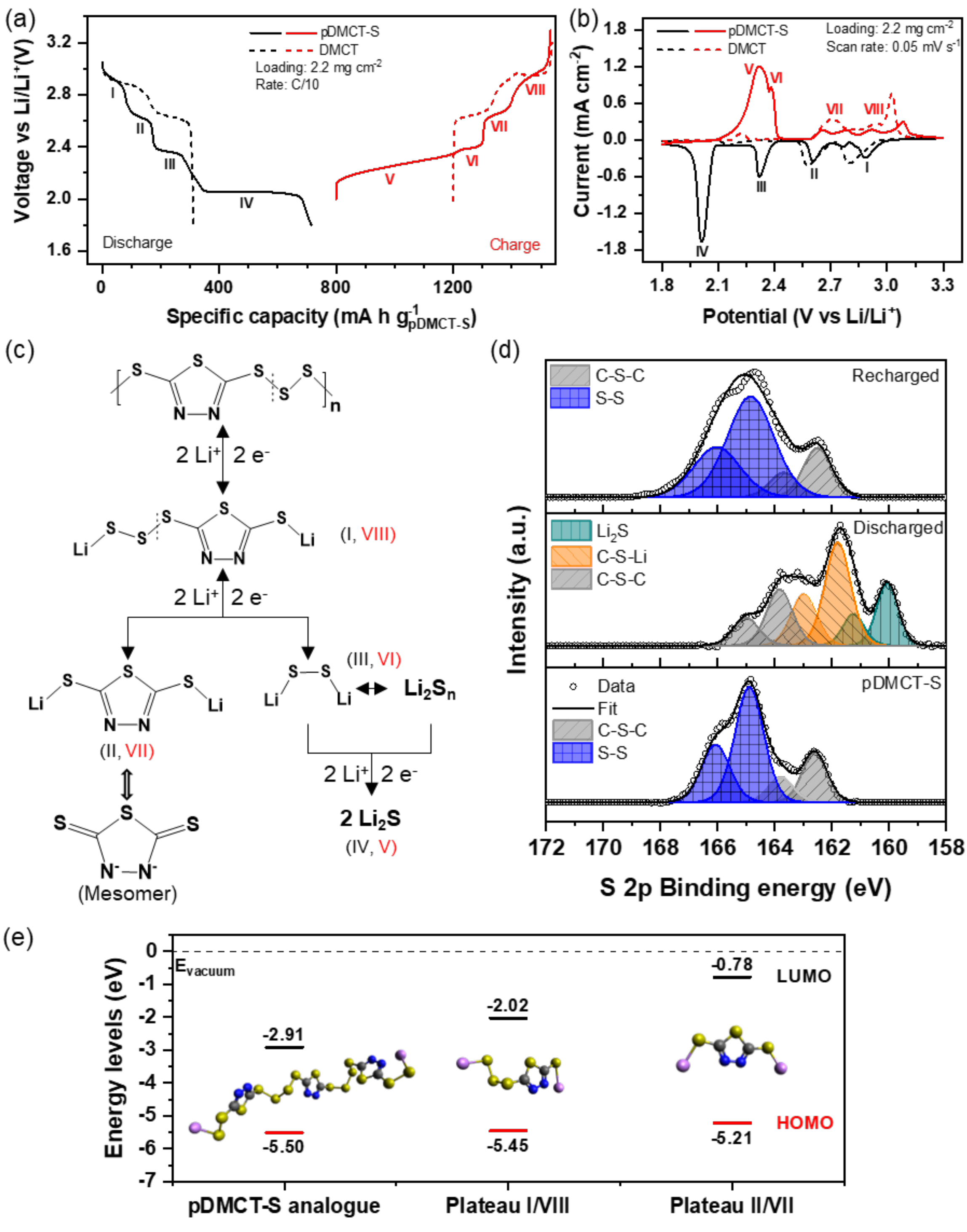

Figure 2. (a) Voltage profiles and (b) CV scans of pDMCT-S and DMCT with Li-metal anode. (c) Scheme showing the expected reaction mechanism during the operation of pDMCT-S. (d) S 2p XPS regions of pristine, discharged, and recharged pDMCT-S cathodes. (e) LUMO/HOMO energy levels of the various intermediates formed during cell cycling.

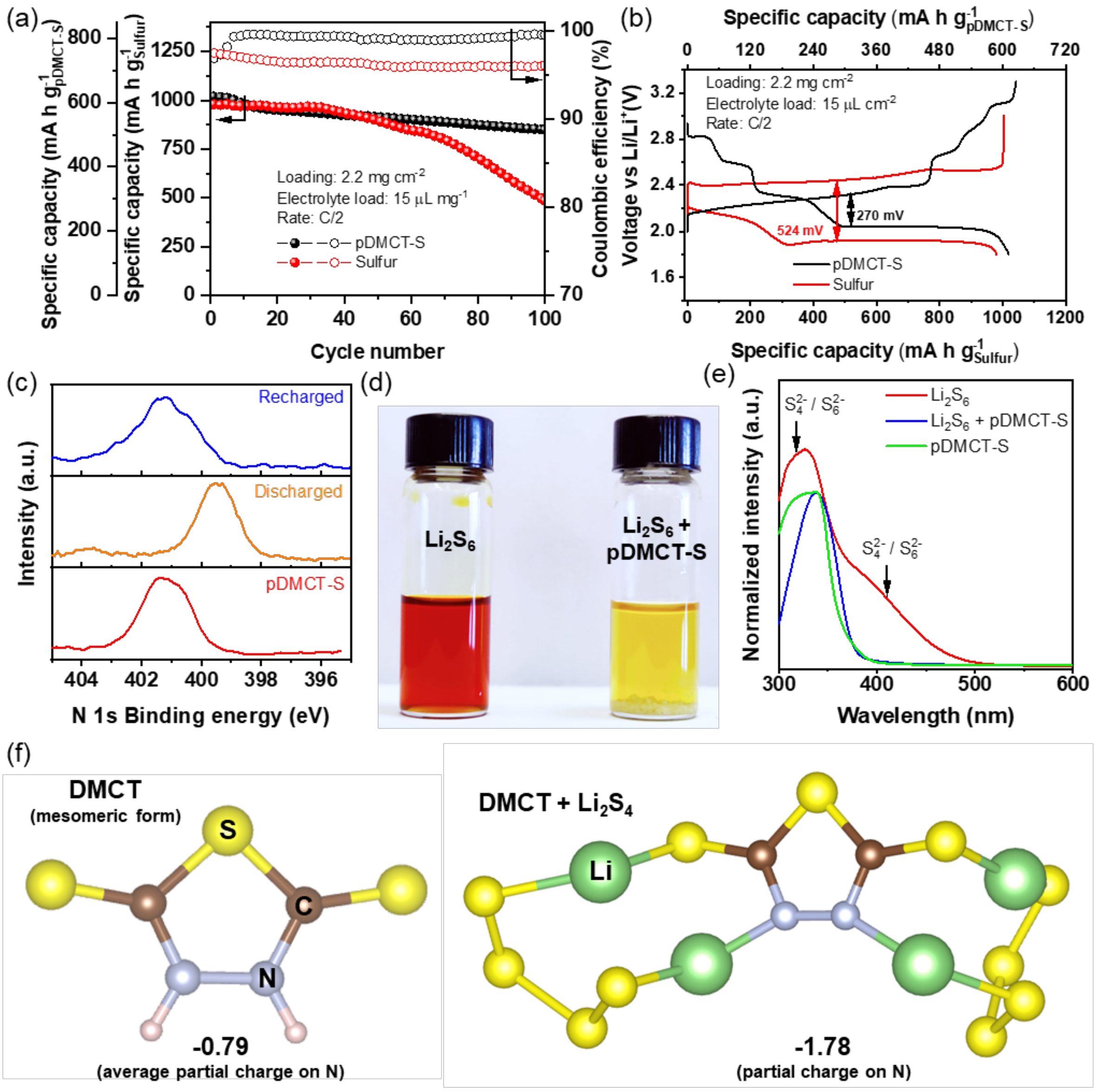

Figure 3. (a) Long-term cycling stability of pDMCT-S and sulfur cathode cycled at C/2 and (b) their representative voltage profiles. (c) N 1s XPS highlighting the oxidation state of nitrogen in the thiadiazole ring during battery cycling. (d) Photograph showing the color change of Li_2S_6 before (left) and after interaction with pDMCT-S (right). (e) UV-Vis analysis of the supernatant from the polysulfide interaction study. (f) Relaxed structures from the AIMD simulations of the mesomeric form of DMCT (left) and on interaction with Li_2S_4. Elements are labeled on the appropriate atoms and the partial charge on the nitrogen in the thiadiazole ring is provided at the bottom.

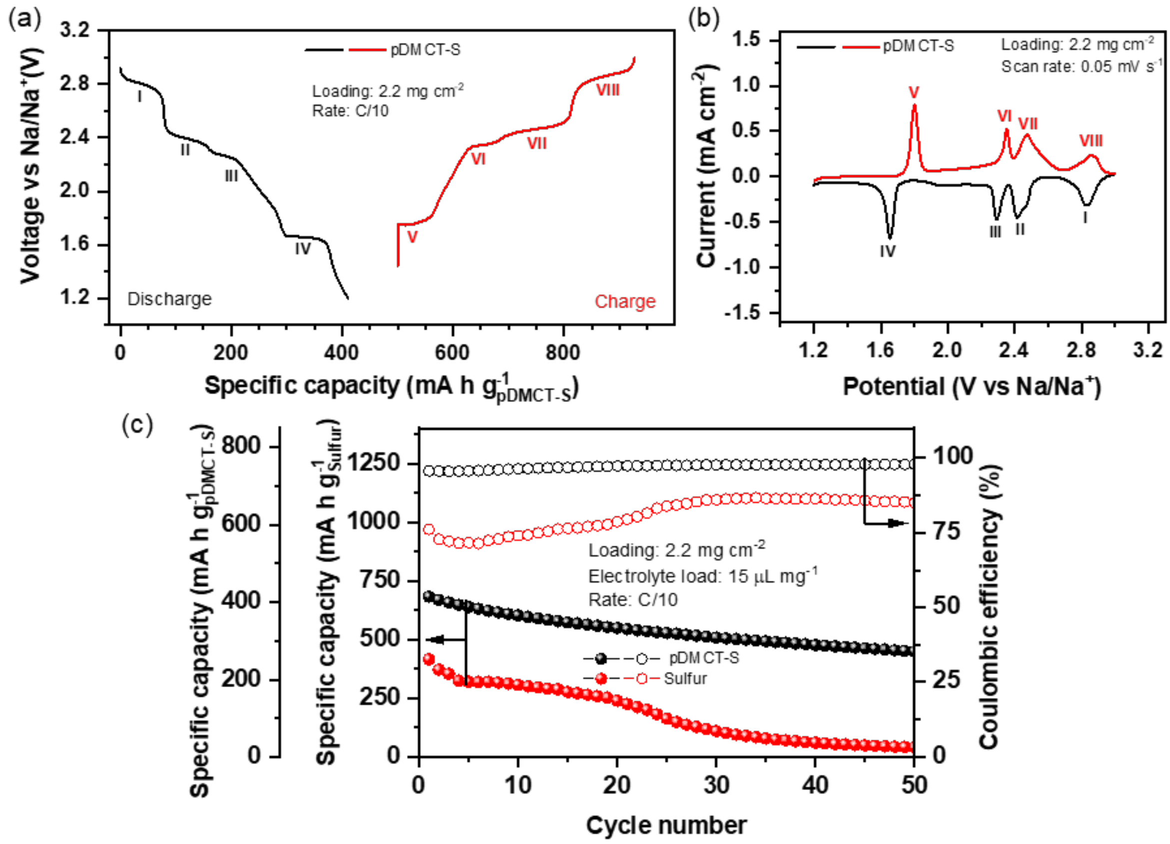

Figure 4. (a) Voltage profile and (b) CV scans of pDMCT-S with Na-metal anode. (c) long-term cycling stability of pDMCT-S and sulfur cathode with a Na-metal anode when cycled at C/10 rate.

ToC Graphic

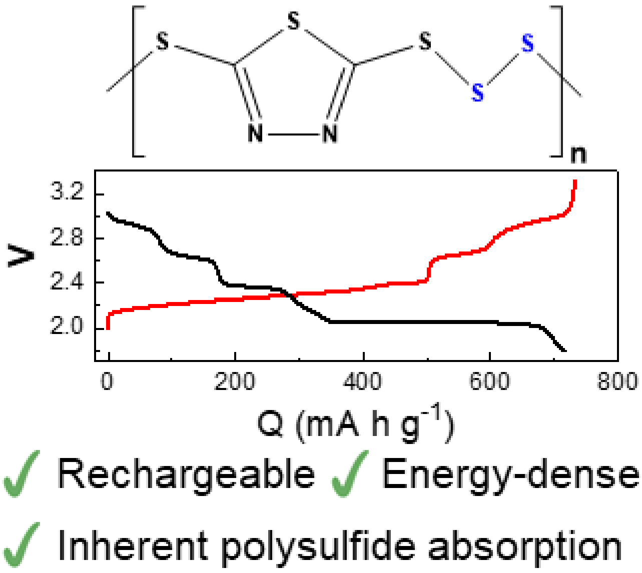

Poly[tetrathio-2,5-(1,3,4-thiadiazole)] or pDMCT-S demonstrates high reversibility in both Li- and Na-metal batteries as the discharge product Li/Na-DMCT can bind to polysulfides. This internal polysulfide sequestration minimizes polysulfide shuttle and mediates the sulfur redox. Consequently, pDMCT-S improves cycling stability as well as capacity compared to sulfur cathodes.

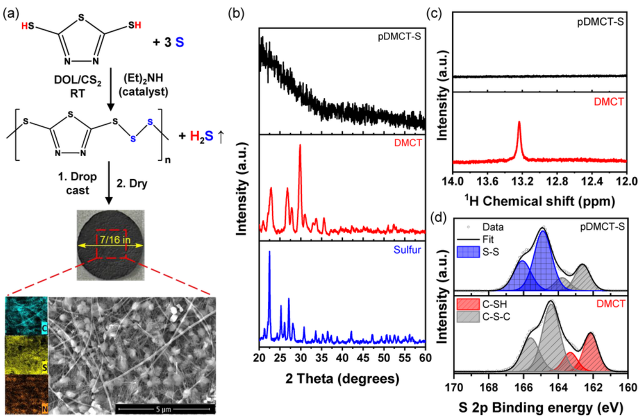

EEM2_12446_Figure 1.tif

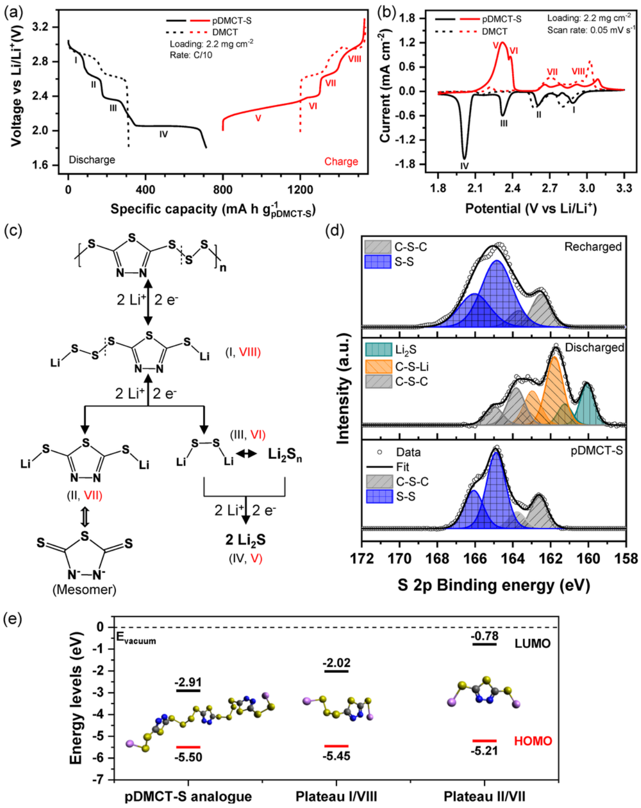

EEM2_12446_Figure 2.tif

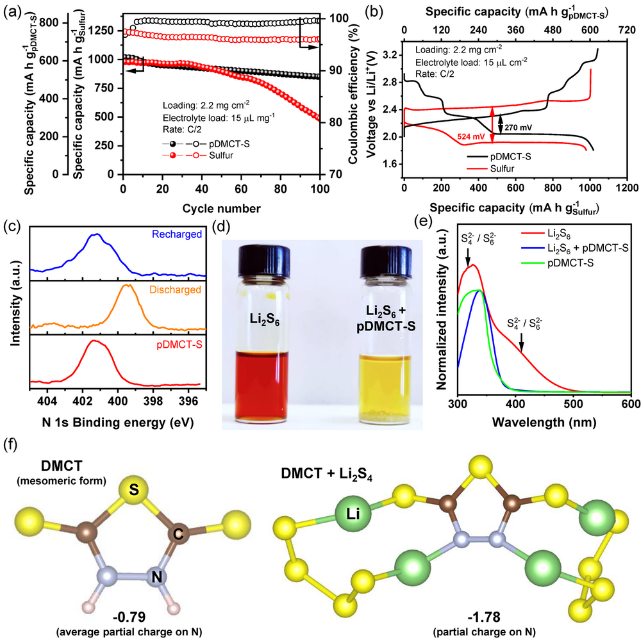

EEM2_12446_Figure 3.tif

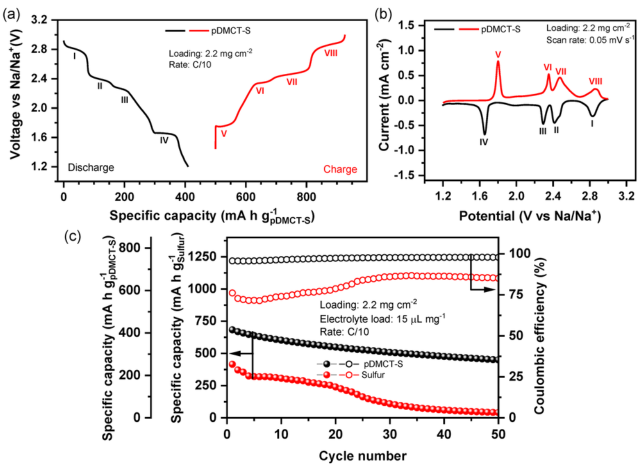

EEM2_12446_Figure 4.tif

EEM-2022-0402

RESPONSE TO REVIEWERS' COMMENTS

REVIEWER 1

General Comment: *The idea of converting the mixture of pDMCT and sulfur into a pDMCT-S polymer is of great interest, however, many scientific concerns should be addressed before this paper can be considered for publication.*

Response to General Comment: We greatly appreciate the positive comments and useful feedback from the reviewer on our work.

Comment 1*: Reaction mechanism of Steps I~III (particularly I and II) proposed in Figure 2c should be confirmed further. Fundamentally, the S-S bonds unlikely form any voltage plateaus higher than 2.5 V (vs. Li). These voltage plateaus (>2.5 V) are very likely related to the redox of the five-member 3,4-thiadiazole ring, other than any S-S bonds.*

Response to Comment 1: We thank the reviewer for this important question. It has been shown that electronegative elements such as nitrogen (*e.g.*, as in thiuram polysulfides[1]), oxygen (*e.g.*, as in xanthogen polysulfides[2]), and phosphorous (*e.g.*, as in 1,4-bis(diphenylphosphanyl) tetrasulfide[3]) withdraw the electron cloud away from the carbon-sulfur bonds in organosulfur compounds. Therefore, such compounds exhibit a voltage plateau > 2.5 V vs Li/Li^+ when the sulfur closest to the electronegative element is lithiated.

Furthermore, seminal studies by Visco *et. al.* and Abruña *et. al.* have shown that the lithiation of the sulfur attached to the thiadiazole ring in DMCT results in a plateau higher than 2.5 V.[4,5] This is further confirmed by the voltage of pure DMCT in Figure 2a. Based on this, we can say that the plateaus labelled I and II in Figure 2a belong to the lithiation of sulfur attached to the thiadazole ring.

Comment 2*: As suggested by the range of the voltage plateaus of Li/pDMCT-S cell in Figure 2a and 2b), the changes in color (Figure 3d) and UV-V absorbance wavelength (Figure 3e) should be due to the chemical redox between Li2S6 and pDMCT-S, forming elemental sulfur and pDMCTLi, other than due to the interaction between the polysulfide anions and pDMCT-S as proposed in this paper.*

Response to Comment 2: We thank the reviewer for raising this critical question. As shown in Figure 3f, two polysulfide molecules can be sequestered by each DMCT molecule. Therefore, the precipitate obtained in the absorption test could consist of Li-DMCT attached to two polysulfide molecules. To further confirm this, we analyzed the precipitate formed in the absorption test with XRD. As seen in **Figure R1**, the precipitate does not show any peaks for sulfur. It does, however, show peaks similar to Li-DMCT albeit with a slight shift. This confirms the ability of pDMCT-S to form structures like those indicated in Figure 3f.

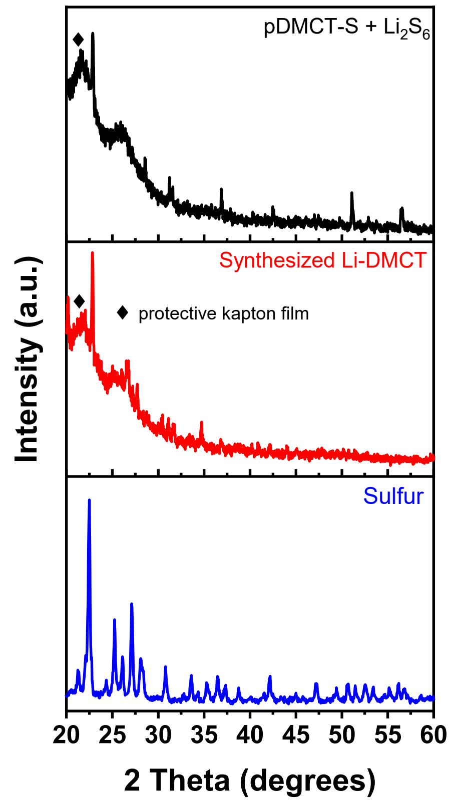

Figure R1. XRD study of the precipitate formed on the interaction of pDMCT-S with lithium polysulfides.

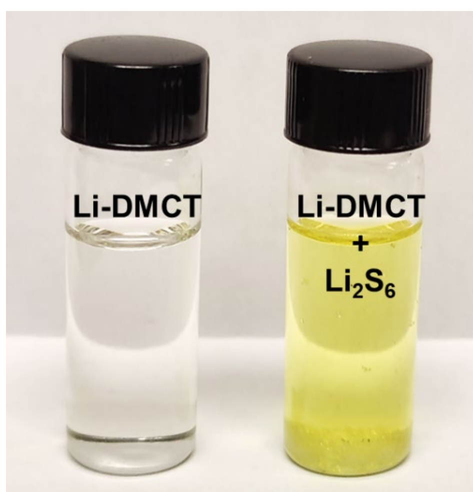

Figure R2. Photograph showing the color change of Li-DMCT before (left) and after interaction with lithium polysulfides (right).

Furthermore, the interaction between lithium polysulfide and Li-DMCT was also studied through an absorption test. As shown in **Figure R2**, the deep-red color of the polysulfides dissipated and a yellow solution was obtained along with yellow-white precipitates. This result is similar to the pDMCT-S – polysulfide absorption test. This suggests that the thiadiazole center is the key to polysulfide absorption.

This data has been added as Figure S8 and S9 in the supporting information, and we have added the appropriate discussion on page 10 of the revised manuscript.

Comment 3*: A common expression for the chemical structure of pDMCT-S polymer in TOC, Figure 1a, and Figure 2c should have all sulfur in one side, like ?(DMCT-S4)?*

Response to Comment 3: We thank the reviewer for pointing out to this discrepancy. We agree with the reviewer that classically, the sulfur is shown on one side while writing the chemical structure. However, authors reporting organosulfur polymers (such as poly-r-S-DIB[6] and poly(S-TATA)[7], for example) usually depict the organic functional group in the center to emphasize the effect of the functional group. We have, therefore, followed a similar style to place an emphasis on the effect of the thiadaizole functional group.

Comment 4*: Once pDMCT-S is fully discharged to pDMCTLi2 and Li2S, can they be reversibly recharged to the original pDMCT-S? Please provide evidence if any.*

Response to Comment 4: We thank the reviewer for raising this important question. XRD analysis was performed on the recharged cathode. As shown in **Figure R3**, the absence of crystalline peaks other than that of the CNT matrix confirms the reformation of the polymer on charge. XPS with Ar^+ sputtering was also performed to further confirm the formation of the polymer on charge.

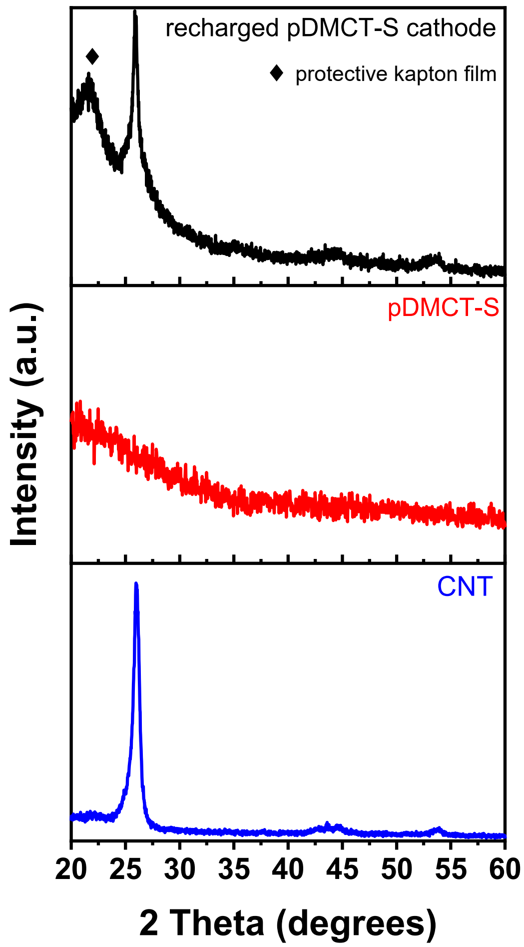

Figure R3. XRD analysis of the pDMCT-S cathode after 1st charge. XRD patterns of electrode components are provided as a reference.

This data has been added as Figure S2b and S3 in the supporting information along with the appropriate discussion on page 8 of the revised manuscript.

Comment 5*: A simile work, https://nam12.safelinks.protection.outlook.com/?url=https%3A%2F%2Fdoi.org%2F10.1002%2Fchem.201103535&data=05%7C01%7C%7C5d5bb0dcebab4ec2593008da24c6e2a8%7C31d7e2a5bdd8414e9e97bea998ebdfe1%7C0%7C0%7C637862733875607018%7CUnknown%7CTWFpbGZsb3d8eyJWIjoiMC4wLjAwMDAiLCJQIjoiV2luMzIiLCJBTiI6Ik1haWwiLCJXVCI6Mn0%3D%7C3000%7C%7C%7C&sdata=X9267qULQLGALKdQW9BaCS83z2TIwJsopOpxV7nmIw4%3D&reserved=0, should be credited.*

Response to Comment 5: We thank the reviewer for highlighting this. The paper suggested by the reviewer was referenced as citation 20 and the contributions of Abruña's group was highlighted on page 3 of the manuscript.

REVIEWER 2

General Comment: *In this manuscript, a DMCT-based material referred to as pDMCT-S has been chosen as cathode with a new four-step redox reaction. The unique mechanism results in an improved performance in Li-S batteries and Na-S batteries, which both prove the wonderful ability of pDMCT-S to limit polysulfides. The results are interesting. However, there are several problems should be clarified.*

Response to General Comments: We thank the reviewer for the positive comments, and we provide the responses to specific questions below.

Comment 1*: How the loading of the electrodes were calculated? Based on the weight of the whole pDMCT-S materials or just the active sulfur elements?*

Response to Comment 1: We thank the reviewer for this important question. The loading of the pDMCT-S/CNT electrodes were calculated based on the total weight of the whole pDMCT-S material. For clarity to the readers, we have reported capacities based on both on the pDMCT-S mass as well as the sulfur mass in the pDMCT-S.

Comment 2*: To further confirm the discharged product, it is better to add XRD result for the discharged cathodes.*

Response to Comment 2: We thank the reviewer for this critical feedback. As suggested by the reviewer, XRD analysis was performed on the discharged cathode as shown in **Figure R4**.

XRD analysis of the discharged cathode suggests that the Li-DMCT is crystalline while the Li_2S is amorphous. This further strengthens the conclusions drawn from XPS studies and validates the reaction mechanism.

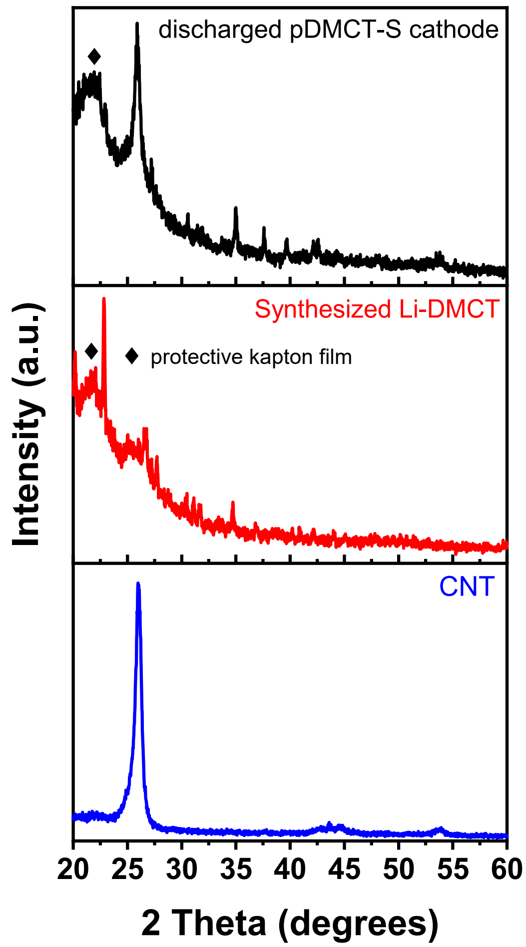

Figure R4. XRD analysis of the pDMCT-S cathode after 1st discharge. XRD patterns of electrode components are provided as a reference.

This data has been included as Figure S2a along with the discussion on page 7 of the revised manuscript.

Comment 3: *Figure 3d-e, please provide the photograph and results of pDMCT-S.*

Response to Comment 3: We thank the reviewer for this question. Photograph of a solution of pDMCT-S in DME/DOL has been included as Figure S6 and is referenced in page 10 of the revised manuscript.

REVIEWER 3

General Comment: *In this manuscript, the authors reported a new organosulfur material as the sulfur-based cathode and study the reaction mechanism. The metal sulfur batteries with such organosulfur cathode showed high capacity and good cycling performance. This work seems interesting, and thus I recommend this manuscript be published after a major revision. To make the conclusions more solid, the following issues should be addressed.*

Response to General Comment: We greatly appreciate the positive comments and useful feedback of the reviewer on our work.

***Comment 1**: It should be noted that the XPS results only revealed the elemental information on the uppermost surface of the sample. Therefore, in the 2.2 section, the area ratio between the neutral sulfur and the heterocyclic sulfur obtained from the XPS results of the cathode surface may not be convincing. Is there any other solid evidence to demonstrate this reaction mechanism?*

Response to Comment 1: We thank the reviewer for this critical comment. We agree with the reviewer that XPS probes only the surface of the sample. To confirm the polymer composition in the depth of the electrode, Ar^+ sputtering was performed on the recharged cathode (**Figure R6**). The area ratio is maintained even after sputtering suggesting uniform distribution of sulfur within the polymer in the bulk of the electrode.

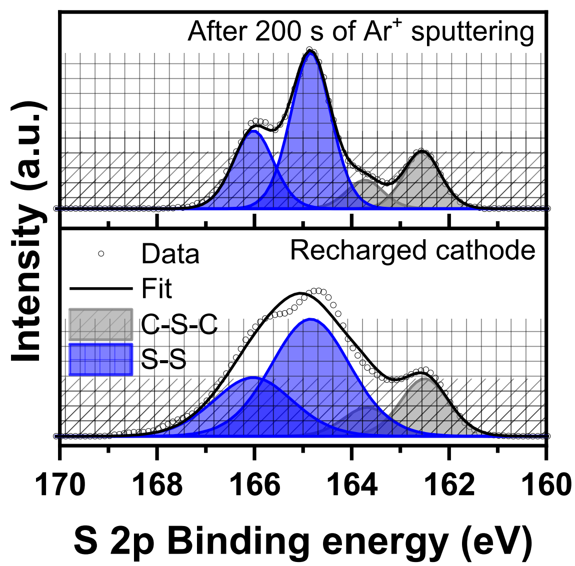

Figure R6. XPS analysis of a recharged pDMCT-S cathode after 200 s of Ar^+ sputtering

Furthermore, XRD analysis was performed as shown in **Figure R7**. The absence of crystalline peaks other than that of the CNT matrix confirms the reformation of the polymer on charge.

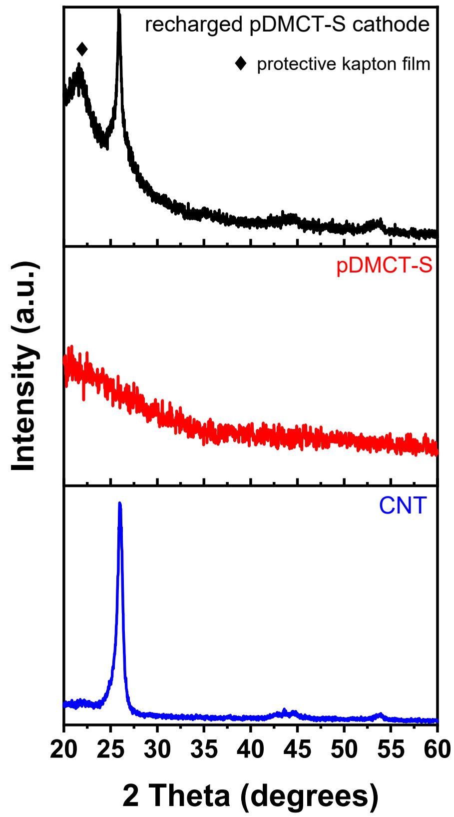

Figure R7. XRD analysis of the pDMCT-S cathode after 1st charge. XRD patterns of electrode components are provided as a reference.

This data has been added as Figure S2b and S3 in the supporting information along with the appropriate discussion on page 8 of the revised manuscript.

Comment 2: *In terms of reaction kinetics, the EIS tests are necessary.*

Response to Comment 2: We thank the reviewer for this critical feedback. We conducted EIS study as per the suggestion of the reviewer. As seen in **Figure R8**, the lowering of charge-transfer resistance in the pDMCT-S cathode when compared to the sulfur cathode corroborates the facile ion- and electron-transport through pDMCT-S.

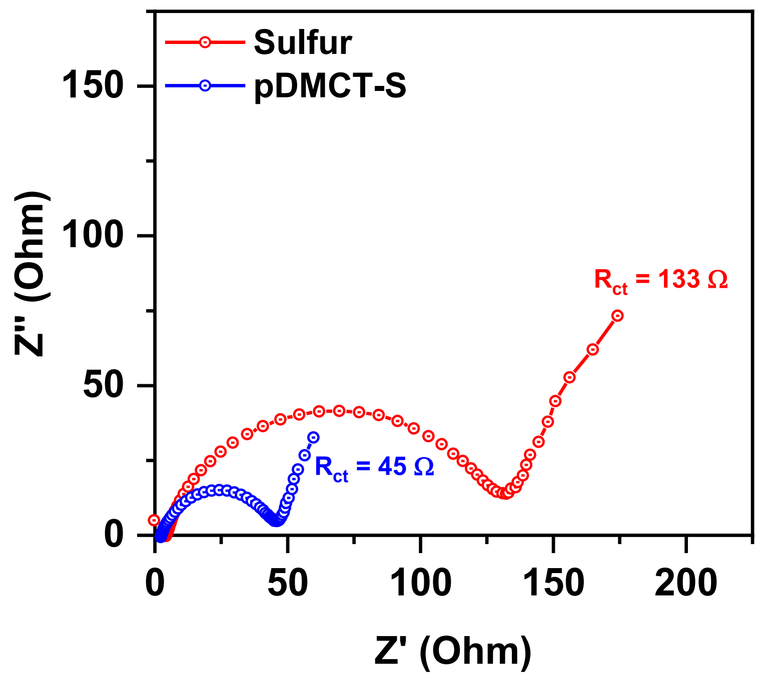

Figure R8. EIS plots of pDMCT-S cathode and sulfur. The charge-transfer resistance (R_{ct}) of each electrode is indicated.

This data has been added as Figure S10 in the supporting information along with the appropriate discussion on page 11 in the revised manuscript.

Comment 3: *In the charge and discharge process, the Gibbs free energy calculations may be necessary, which can be obtained from the DFT calculation. Explaining this would increase the intuitive understanding of the reaction mechanism and the advantages of such cathode.*

Response to Comment 3: We thank the reviewer for this valuable suggestion. The treatment of polymers and free lithium metal as a part of calculating the Gibbs free energy using DFT/AIMD results in ambiguous values. It has been shown that calculation of the lowest unoccupied molecular orbital (LUMO) and highest occupied molecular orbital (HOMO) energy levels is an accurate descriptor of reaction mechanism and the viability of reaction intermediates in organic molecules especially organopolysulfides.[1,7–9] Therfore, these calcualtions were performed as shown in **Figure R9**.

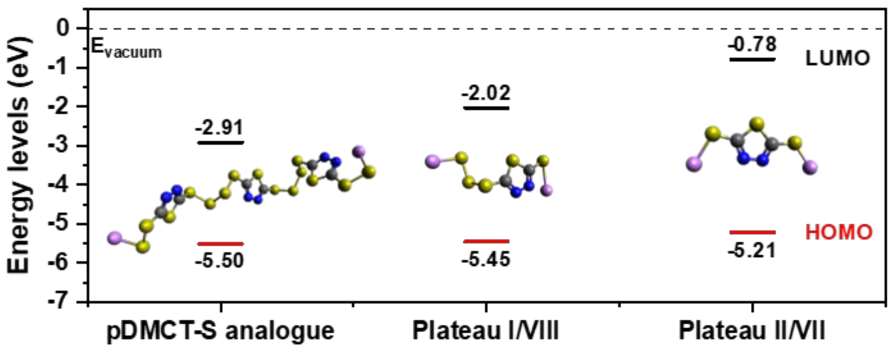

Figure R9. LUMO/HOMO energy levels of the various intermediates formed during battery cycling.

The DFT calculation shows that as we go from pDMCT-S to Li-DMCT, there is an increase in the LUMO/HOMO levels. This suggests that the intermediates considered in the scheme shown in Figure 2c are viable and energy of formation of these intermediates is favorable (*i.e.* $\Delta G < 0$). The gradual increase also corroborates the stepwise lithiation of pDMCT-S.

This data has now been included in Figure 2e and discussed on page 8 in the revised manuscript

Comment 4: *In the 2.3 section, it is emphasized that the pDMCT-S can effectively encapsulate the lithium polysulfides within the polymer. In addition to electrochemical results, it would be interesting to develop post-mortem analysis of the cathode, membranes, or lithium anode used in Figure 3a. This would provide a better understanding.*

Response to Comment 4: We thank the reviewer for this critical feedback. We have now performed SEM analysis of the cycled anodes as shown in **Figure R10**. We can see that the unregulated polysulfide shuttle from the sulfur cathode results in mossy and dendritic Li deposits. On the other hand, the reduction in polysulfide migration results in smoother Li deposits.

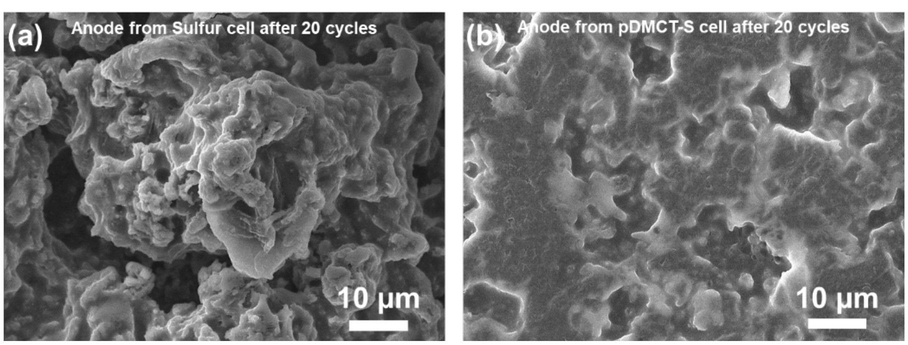

Figure R10. SEM micrographs of the Li-metal anodes from cell with (a) sulfur cathode and (b) pDMCT-S cathode.

This data has been added as Figure S12 in the supporting information along with the appropriate discussion on pages 11 and 12 in the revised manuscript.

References

[1] A. Bhargav, Y. Ma, K. Shashikala, Y. Cui, Y. Losovyj, Y. Fu, *J. Mater. Chem. A* **2017**, *5*, 25005.

[2] A. Bhargav, A. Manthiram, *Adv. Energy Mater.* **2020**, *10*, 2001658.

[3] D. Y. Wang, Y. Si, W. Guo, Y. Fu, *Nat. Commun. 2021 121* **2021**, *12*, 1.

[4] M. Liu, S. J. Visco, L. C. De Jonghe, *J. Electrochem. Soc.* **1989**, *136*, 2570.

[5] J. Gao, M. A. Lowe, S. Conte, S. E. Burkhardt, H. D. Abruña, *Chem. – A Eur. J.* **2012**, *18*, 8521.

[6] A. G. Simmonds, J. J. Griebel, J. Park, K. R. Kim, W. J. Chung, V. P. Oleshko, J. Kim, E. T. Kim, R. S. Glass, C. L. Soles, Y.-E. Sung, K. Char, J. Pyun, *ACS Macro Lett.* **2014**, *3*, 229.

[7] H. Kang, H. Kim, M. J. Park, *Adv. Energy Mater.* **2018**, *8*, 1802423.

[8] Z. Song, Y. Qian, X. Liu, T. Zhang, Y. Zhu, H. Yu, M. Otani, H. Zhou, *Energy Environ. Sci.* **2014**, *7*, 4077.

[9] M. Zhao, X.-Y. Li, X. Chen, B.-Q. Li, S. Kaskel, Q. Zhang, J.-Q. Huang, *eScience* **2021**, *1*, 44.

ToC

Poly[tetrathio-2,5-(1,3,4-thiadiazole)] or pDMCT-S demonstrates high reversibility in both Li- and Na-metal batteries as the discharge product Li/Na-DMCT can bind to polysulfides. This internal polysulfide sequestration minimizes polysulfide shuttle and mediates the sulfur redox. Consequently, pDMCT-S improves cycling stability as well as capacity compared to sulfur cathodes.

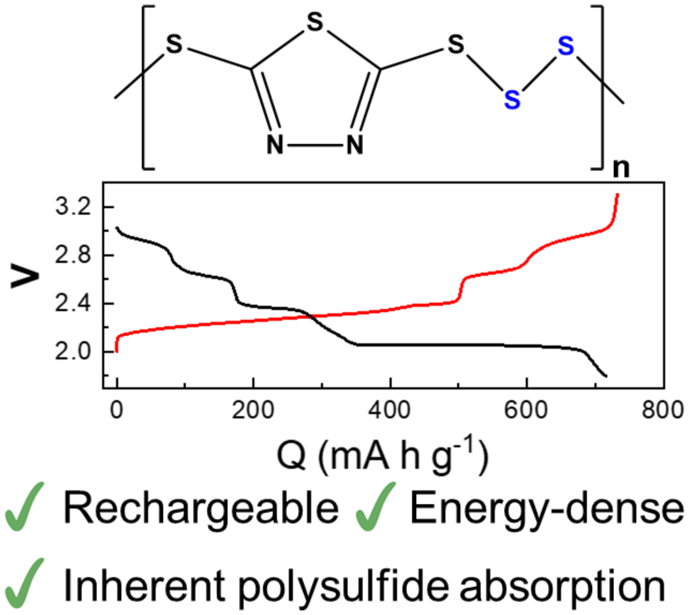

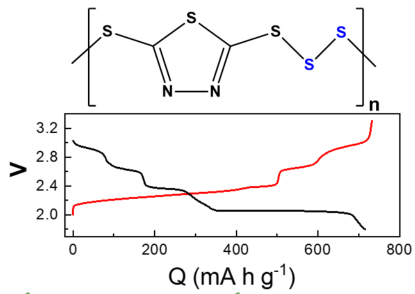

✓ Rechargeable ✓ Energy-dense

✓ Inherent polysulfide absorption

EEM2_12446_ToC.tif